Electronic Supplementary Information

Synthesis, crystal structure and magnetism of new salicylamidoxime-based hexanuclear manganese(III) single-molecule magnets†

José Martínez-Lillo,[a] Adrian-Raul Tomsa,[‡a] Yanling Li,[a] Lise-Marie Chamoreau,[a] Eduard Cremades,[b] Eliseo Ruiz,[b] Anne-Laure Barra,[c] Anna Proust,[a,d] Michel Verdaguer*[a] and Pierre Gouzerh*[a]

[a] Institut Parisien de Chimie Moléculaire, UMR CNRS 7201, UPMC Univ Paris 06, Case courrier 42, 4 Place Jussieu, 75252 Paris Cedex 05, France. E-mail: michel.verdaguer@upmc.fr, pierre.gouzerh@upmc.fr

[b] Department of Inorganic Chemistry, University of Barcelona, Diagonal 647, 08028 Barcelona, Spain

[c] LNCMI-CNRS B.P. 146, 38042 Grenoble Cedex 9, France

[d] Institut Universitaire de France, 103 Boulevard Saint Michel, 75003 Paris, France

1. Crystal data: Table S1 2

2. Magnetic data: Figures S1-S33 3-11

3. High field EPR study of 2': Figures S34-36 12-14

1. Crystal data

Table S1. Unit cell parameters for compounds **9-13**

	a / Å	*b* / Å	*c* / Å	*α* / °	*β* / °	*γ* / °	*V*/ Å^3	Space group
9	12.321(1)	13.722(1)	32.529(4)	101.553(7)	89.916(9)	111.921(7)	4982.4(8)	*P*(-1)[a]
10	10.7716(19)	13.562(2)	13.6380(8)	81.856(7)	85.189(7)	66.720(12)	1810.7(5)	*P*(-1)
11	11.6917(17)	13.2207(11)	17.404(2)	82.892(9)	76.7521(11)	81.328(9)	2577.5(6)	*P*(-1)
12	19.652(9)	31.131(4)	36.125(6)	90	92.27(2)	90	22084(7)	$P2_1/n$
13	12.6802(12)	12.7372(15)	13.4047(11)	65.120(7)	70.487(7)	63.767(3)	1732.4(3)	*P*1

[a] Two independent molecules in the unit cell.

2. Magnetic data

Magnetic data for compounds **1** and **2** have been reported previously (A.-R. Tomsa et al., Chem. Commun., 2010, 46, 5106-5108. DOI: 10.1039/c0cc00458e.

2.1. Magnetic data for $[Mn_6(\mu_3\text{-}O)_2(PhCO_2)_2(H_2N\text{-}saoH_2)_6(EtOH)_6]\cdot EtOH]\cdot H_2O$ (2'')

$\chi_M T$ vs T for **2''** (see text, Fig. 4)

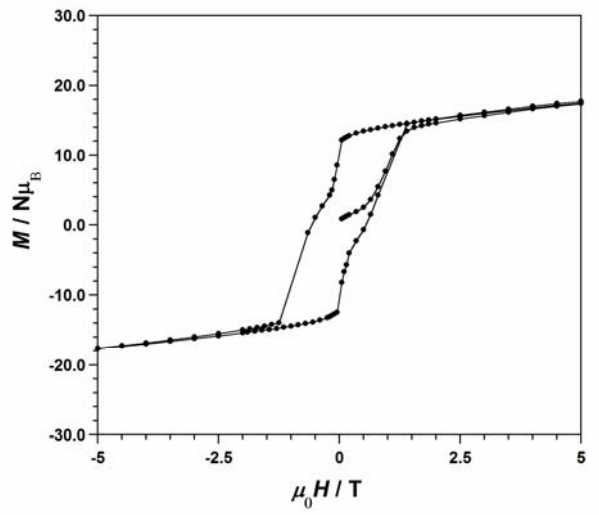

Fig. S1 Magnetization *vs* field hysteresis loop for **2"** at 2 K

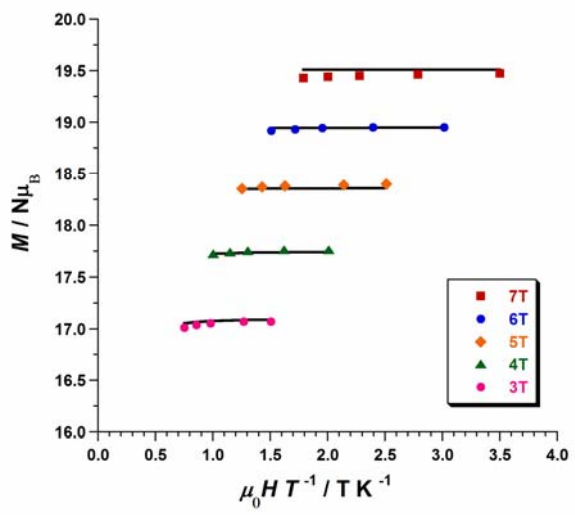

Fig. S2 Magnetization vs H/T for **2"**

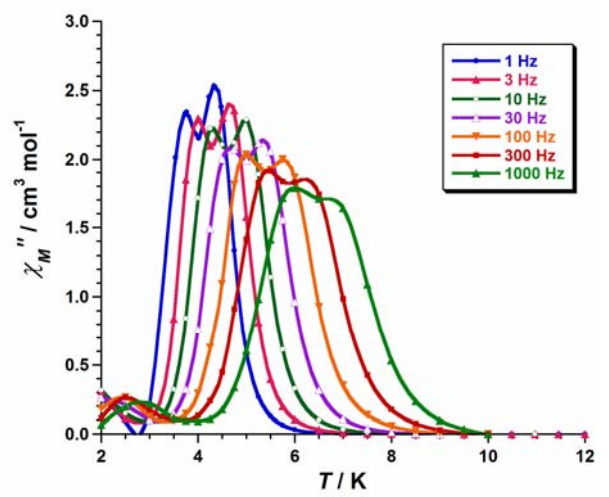

Fig. S3 Out-of-phase χ_M" *ac* susceptibility for **2''**

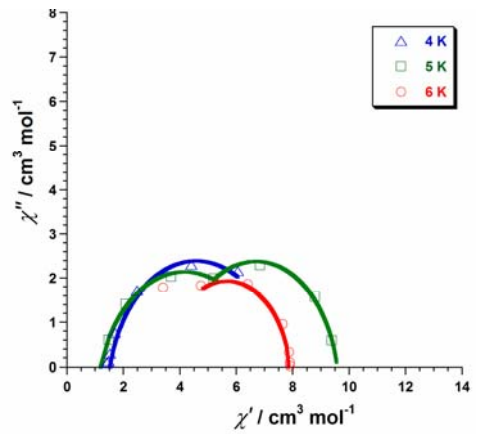

Fig. S4 Out-of-phase *vs* in-phase *ac* susceptibility for **2''**

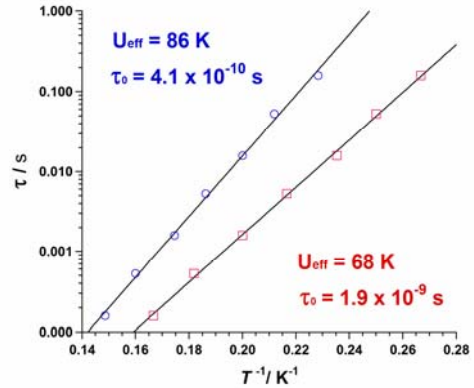

Fig. S5 Arrhenius plots for the two relaxation processes of **2''**.

2.2. Magnetic data for $[Mn_6O_2(PhCO_2)_2(H_2N$ $sao)_6(EtOH)_6]\cdot 4EtOH$ (3')

Sample introduction in the SQUID at 200 K

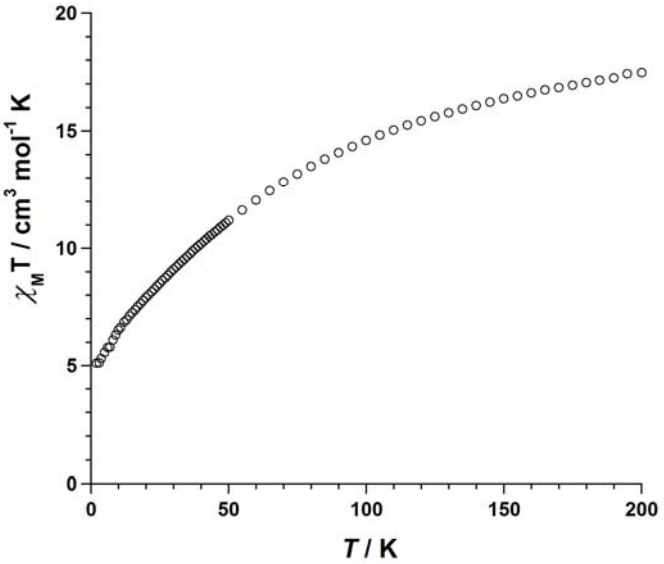

Fig. S6 $\chi_M T$ vs T for **3'**

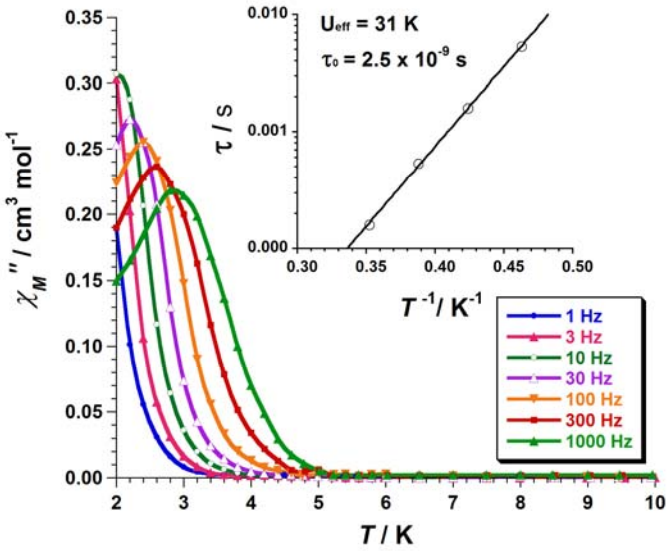

Fig. S7 Out-of-phase χ_M'' *ac* susceptibility and Arrhenius plot for **3'**

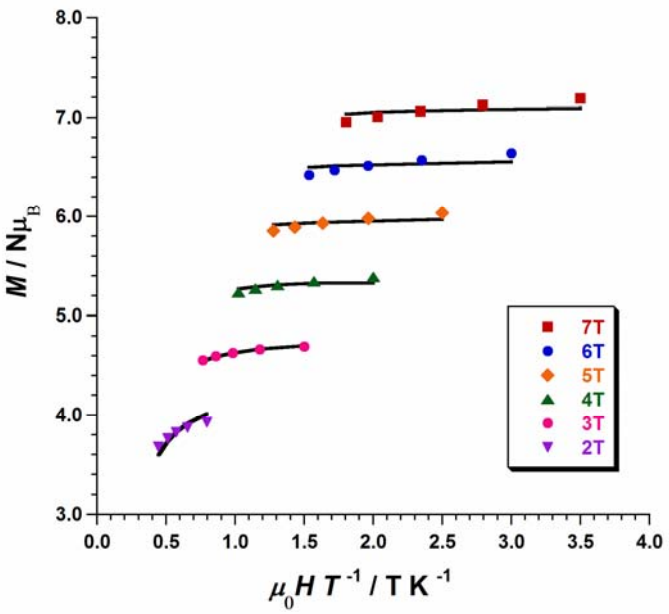

Fig. S8 Magnetization *vs* H/T for **3'**

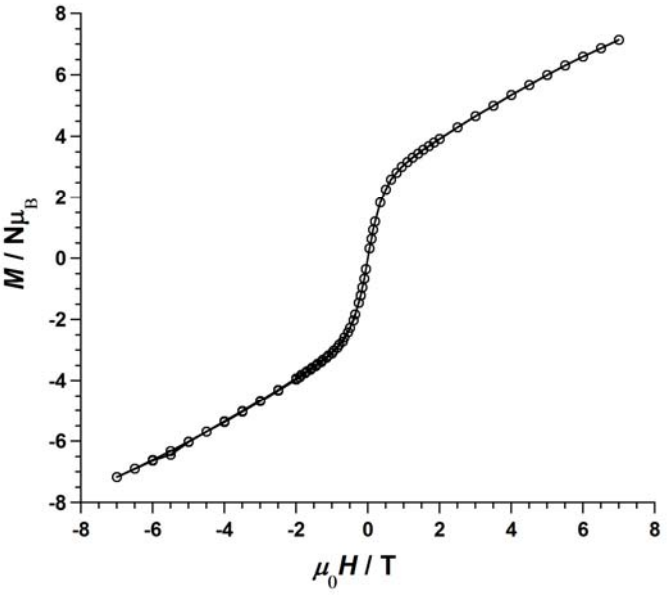

Fig. S9 Magnetization *vs* Field loop for **3'** at 2 K

2.3. Magnetic data for $[Mn_6(\mu_3\text{-}O)_2(PhCO_2)_2(H_2N\text{-}sao)_6(i\text{PrOH})_4(EtOH)_2]\cdot 4i\text{PrOH}$ (4)

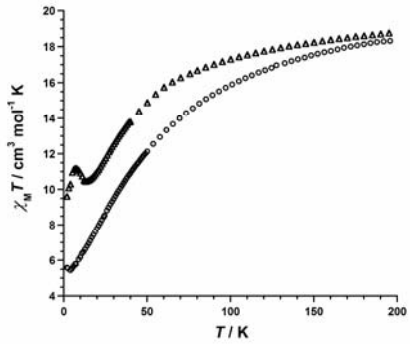

Fig. S10 $\chi_M T$ *vs* T for **4** (o: introduction at 200 K; Δ: introduction at 300 K)

Sample introduction at 200 K

Sample introduction at 300 K

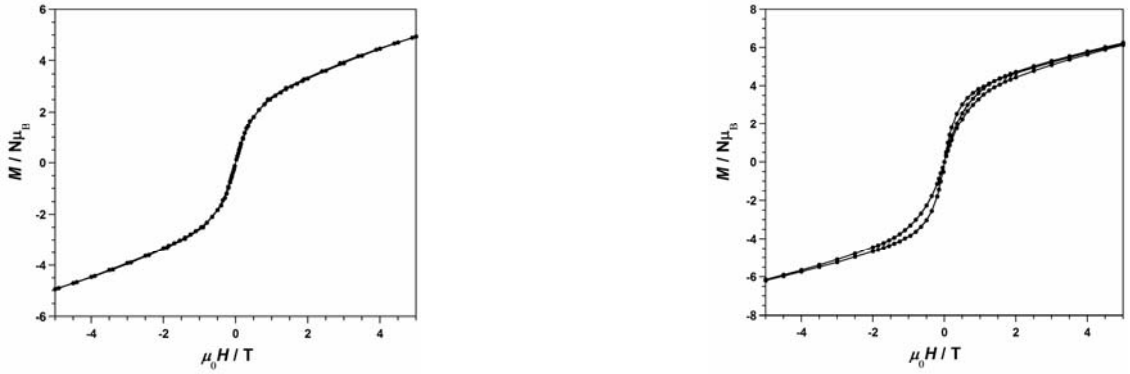

Fig. S11 Magnetization *vs* field loops for **4** at 2 K

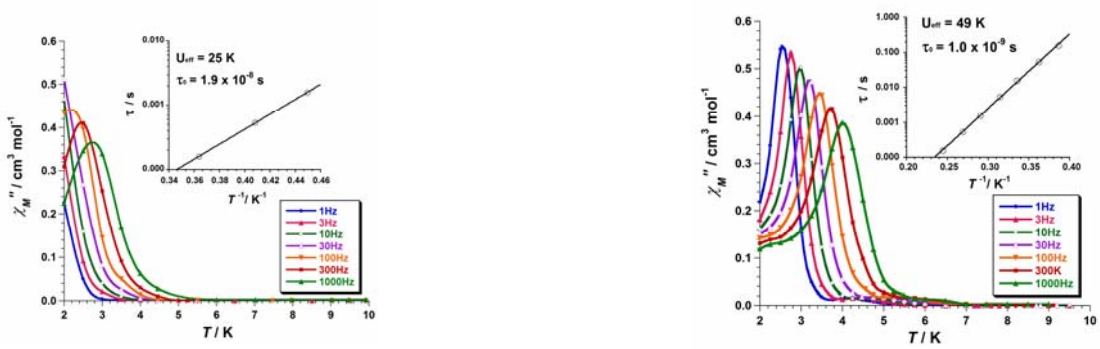

Fig. S12 Out-of-phase *ac* susceptibility and Arrhenius plots for **4**

Fig. S13 Out-of-phase *vs* in-phase *ac* susceptibility for **4**

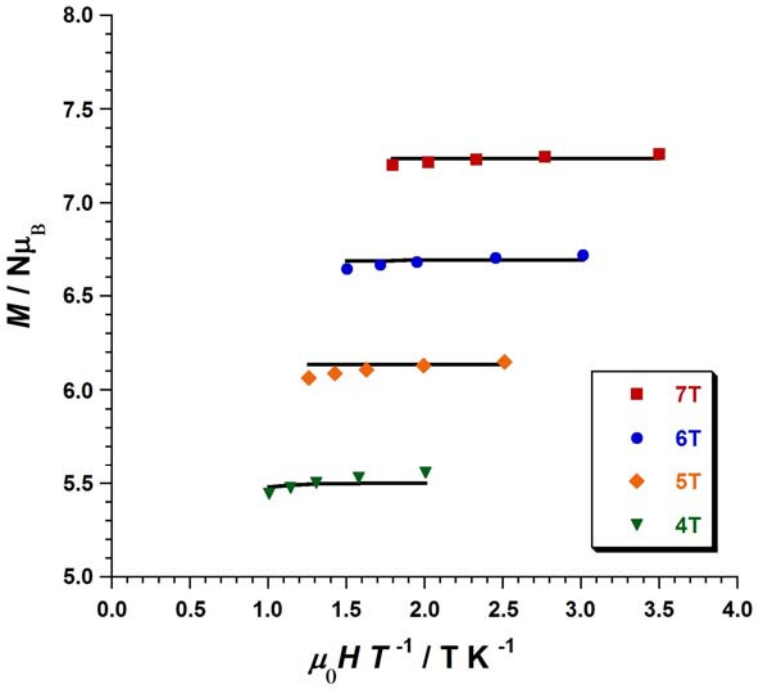

Fig. S14 Magnetization *vs* H/T for **4**

2.4. Magnetic data for $[Mn_6O_2(tBuCO_2)_2(H_2N\text{-}sao)_6(EtOH)_6]\cdot 5EtOH$ (5)

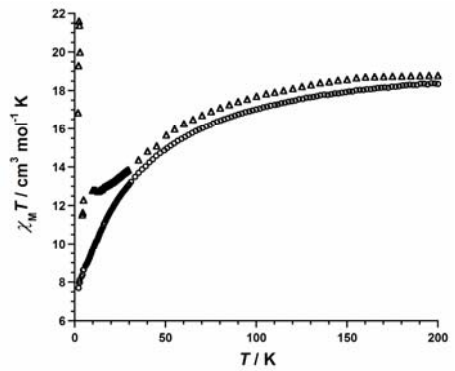

Fig. S15 $\chi_M T$ *vs* *T* for **5** (o: introduction at 200 K; Δ: introduction at 300 K)

Sample introduction at 200 K

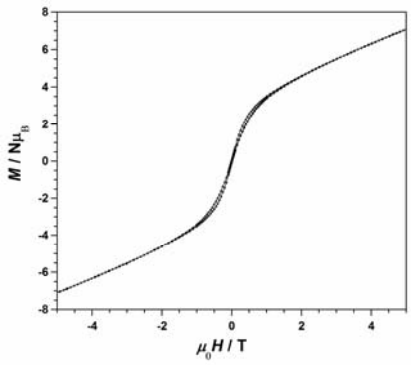

Sample introduction at 300 K

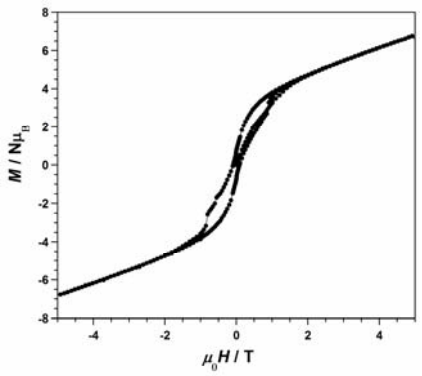

Fig. S16 Magnetization *vs* field loops for **5** at 2 K

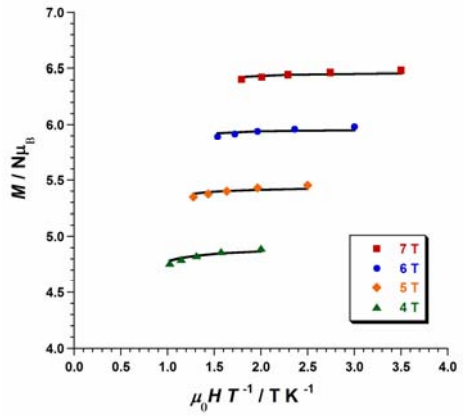

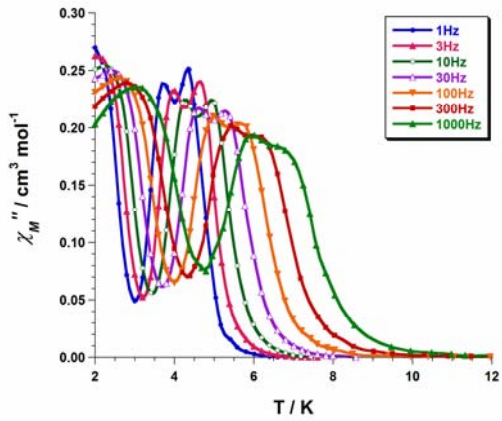

Fig. S17 Out-of-phase *ac* susceptibility for **5**

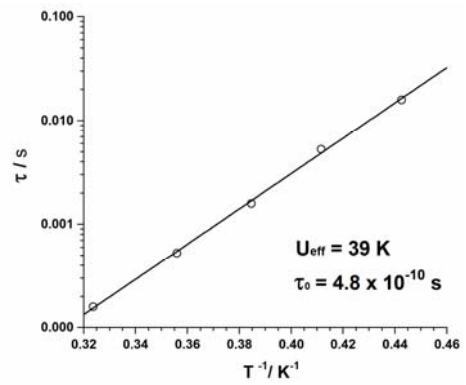

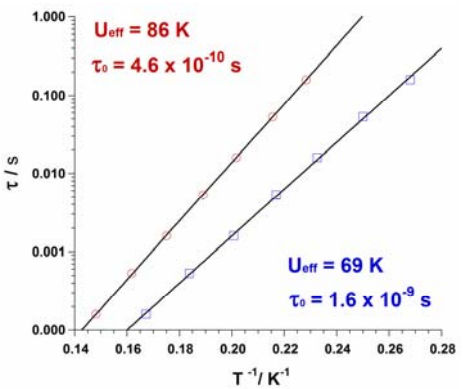

Fig. S18 Arrhenius plots for **5**

2.5. Magnetic data for $[Mn_6(\mu_3\text{-}O)_2\{C_6H_4(O)CN\}_2(H_2N\text{-}sao)_6(EtOH)_6]\cdot 4H_2O$ (6)

Sample introduction at 200 K

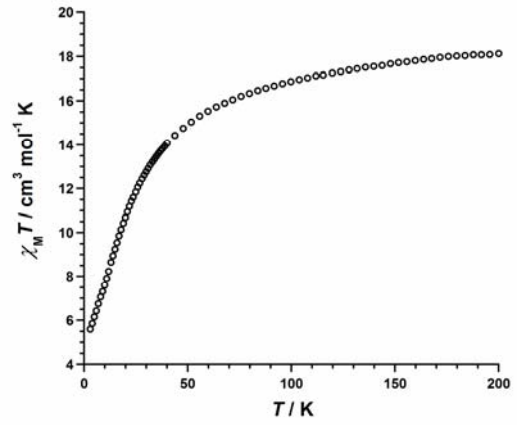

Fig. S19 $\chi_M T$ *vs* T for **6**

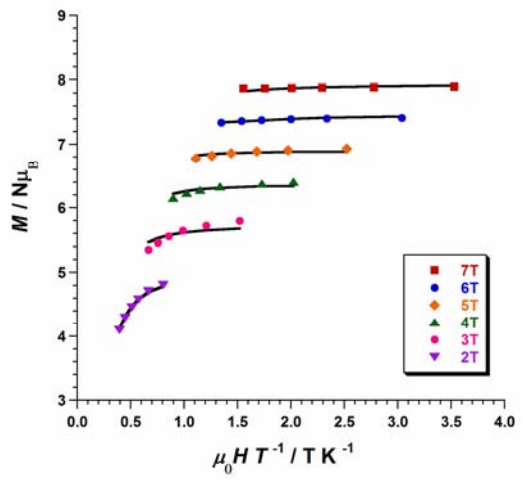

Fig. S20 Magnetization *vs* H/T for **6**

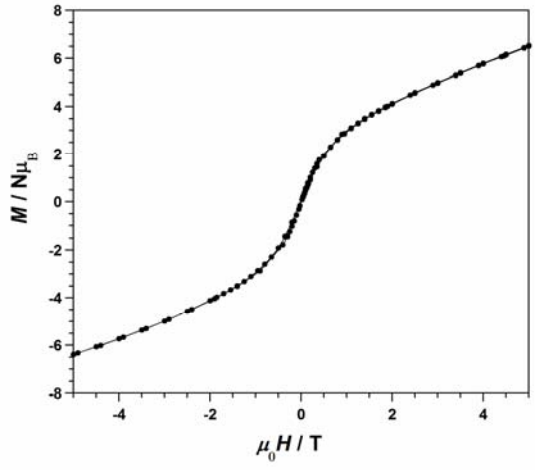

Fig. S21 Magnetization *vs* field loop for **6**

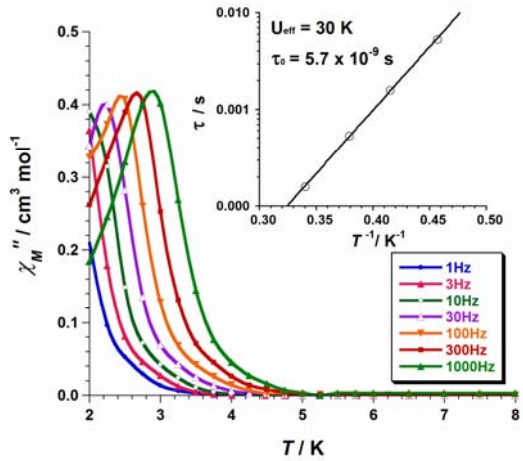

Fig. S22 Out-of-phase *ac* susceptibility for **6**

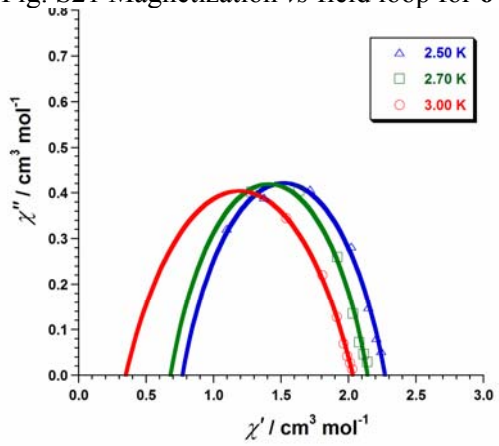

Fig. S23 Out-of-phase *vs* in-phase *ac* susceptibility for **6**

2.6. Magnetic data for $[Mn_6(\mu_3\text{-}O)_2(H_2N\text{-}sao)_6(MeOH)_8]Cl_2\cdot 9MeOH$ (7)

Sample introduction at 200 K

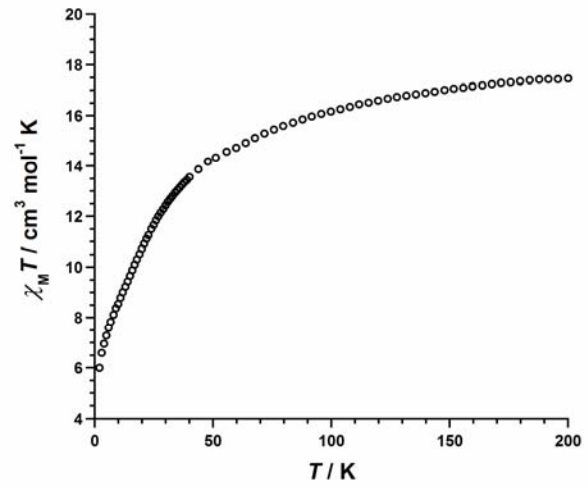

Fig. S24 $\chi_M T$ *vs* T for **7**

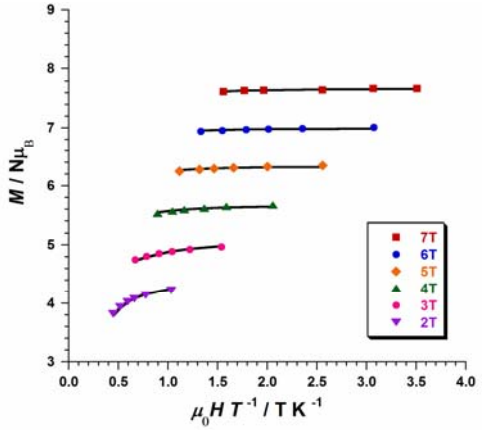

Fig. S25 Magnetization *vs* H/T for **7**

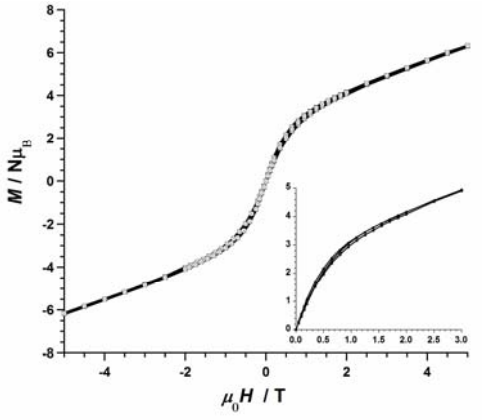

Fig. S26 Magnetization *vs* field loop for **7** at 2 K

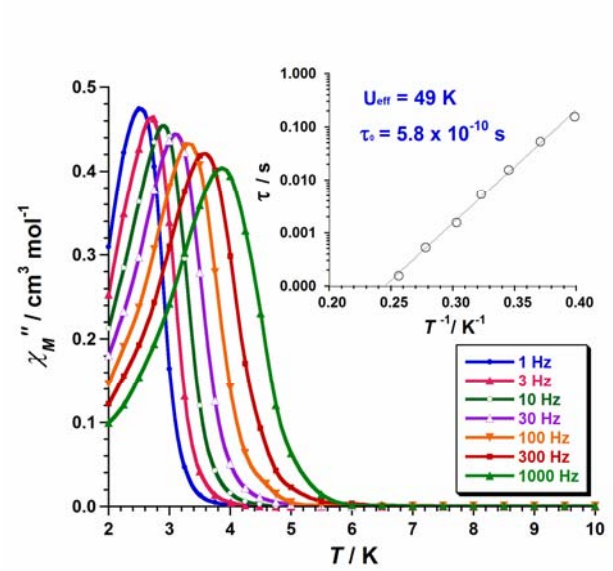

Fig. S27 Out-of-phase *ac* susceptibility for **7**

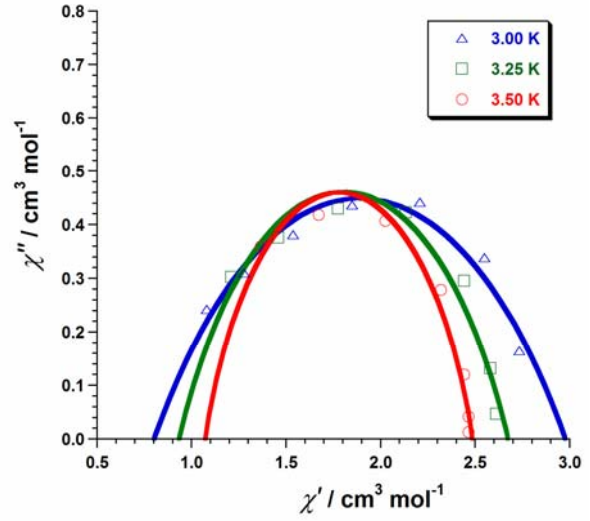

Fig. S28 Out-of-phase *vs* in-phase *ac* susceptibility for **7**

2.7 Magnetic data for $[Mn_6(\mu_3\text{-}O)_2Cl_2(H_2N\text{-}sao)_6(EtOH)_4(H_2O)_2]\cdot 5\ EtOH$ (8)

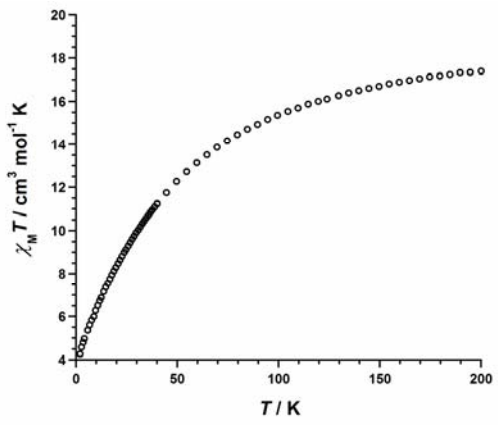

Fig. S29 $\chi_M T$ *vs* T for **8**

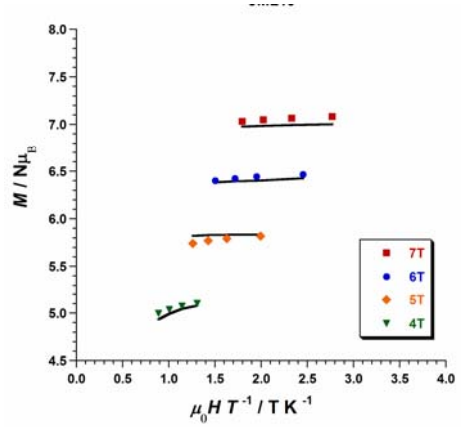

Fig. S30 Magnetization *vs* H/T for **8**

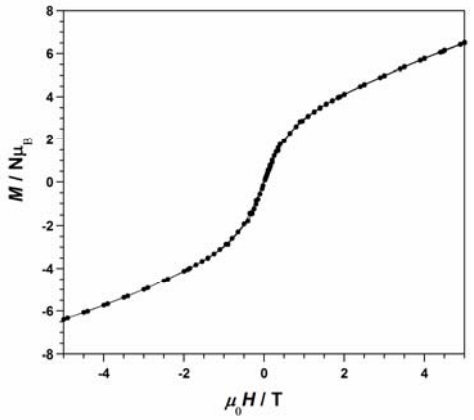

Fig. S31 Magnetization *vs* field loop for **8**

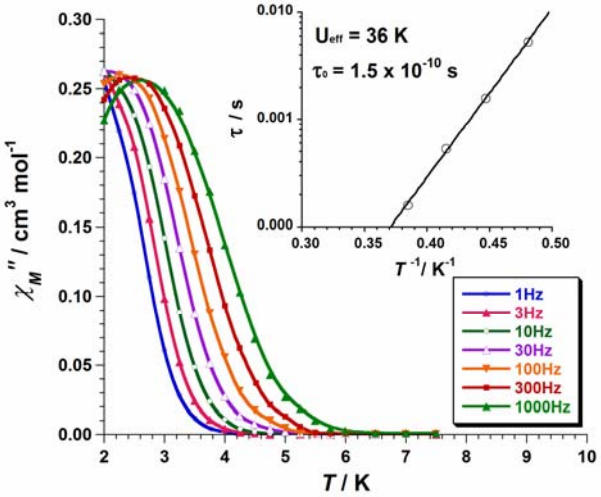

Fig. S32 Out-of-phase *ac* susceptibility and Arrhenius plot for **8**

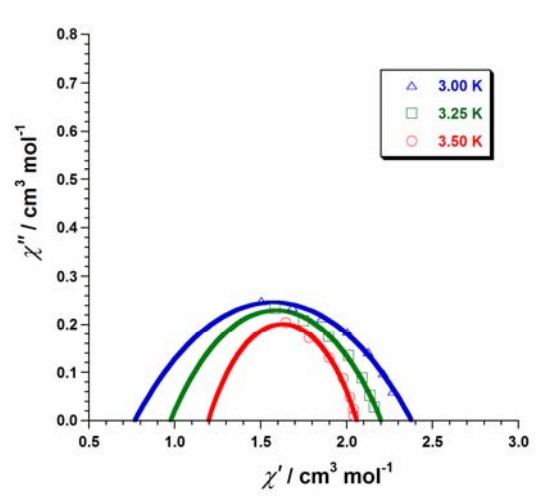

Fig. S33 Out-of-phase *vs* in-phase *ac* susceptibility for **8**

3. High field EPR study of 2' (pellet sample)

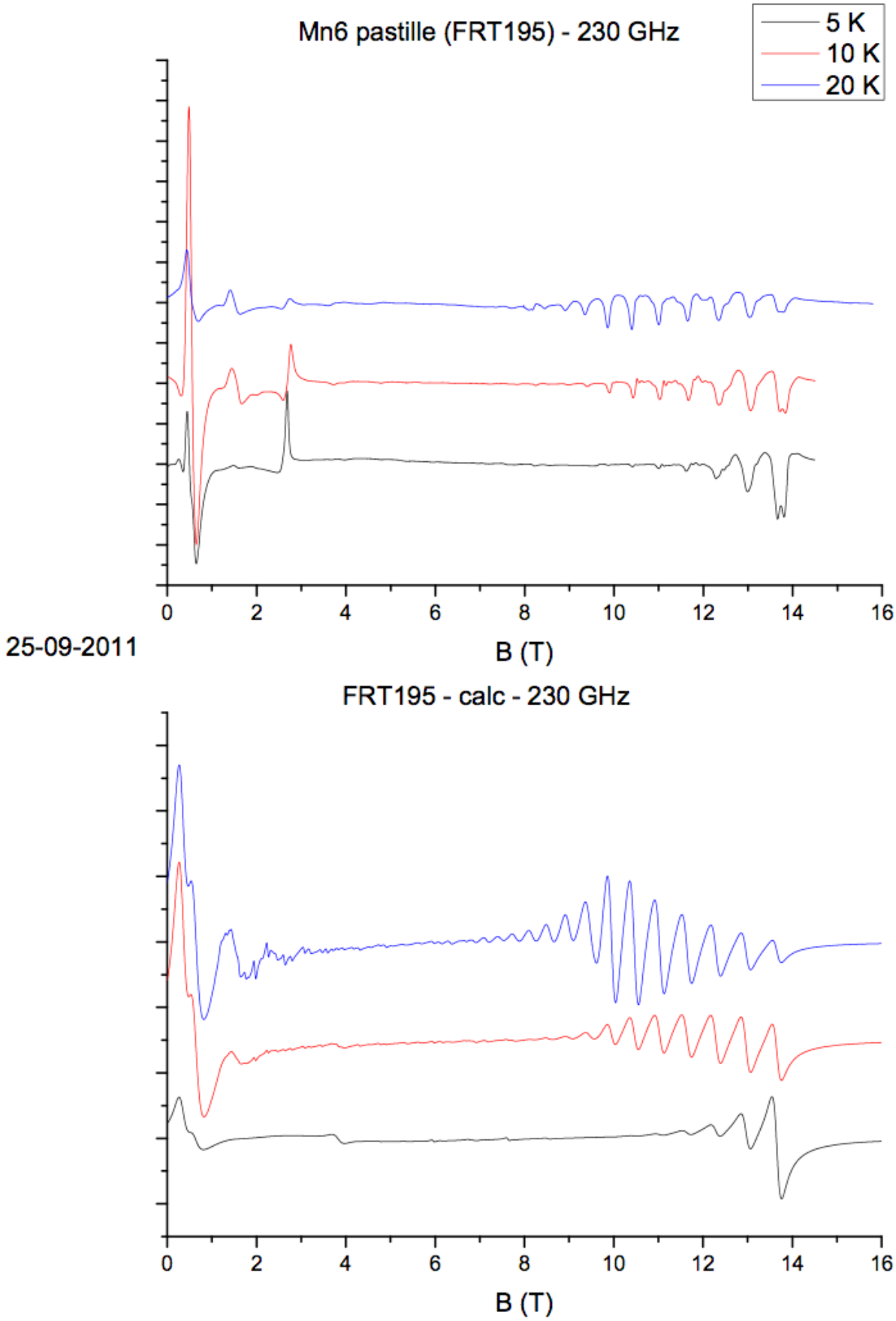

Fig. S34 Experimental (top) and calculated spectra for an $S = 12$ ground state (bottom) of **2'** at 230 GHz and T = 5, 10 et 20 K.

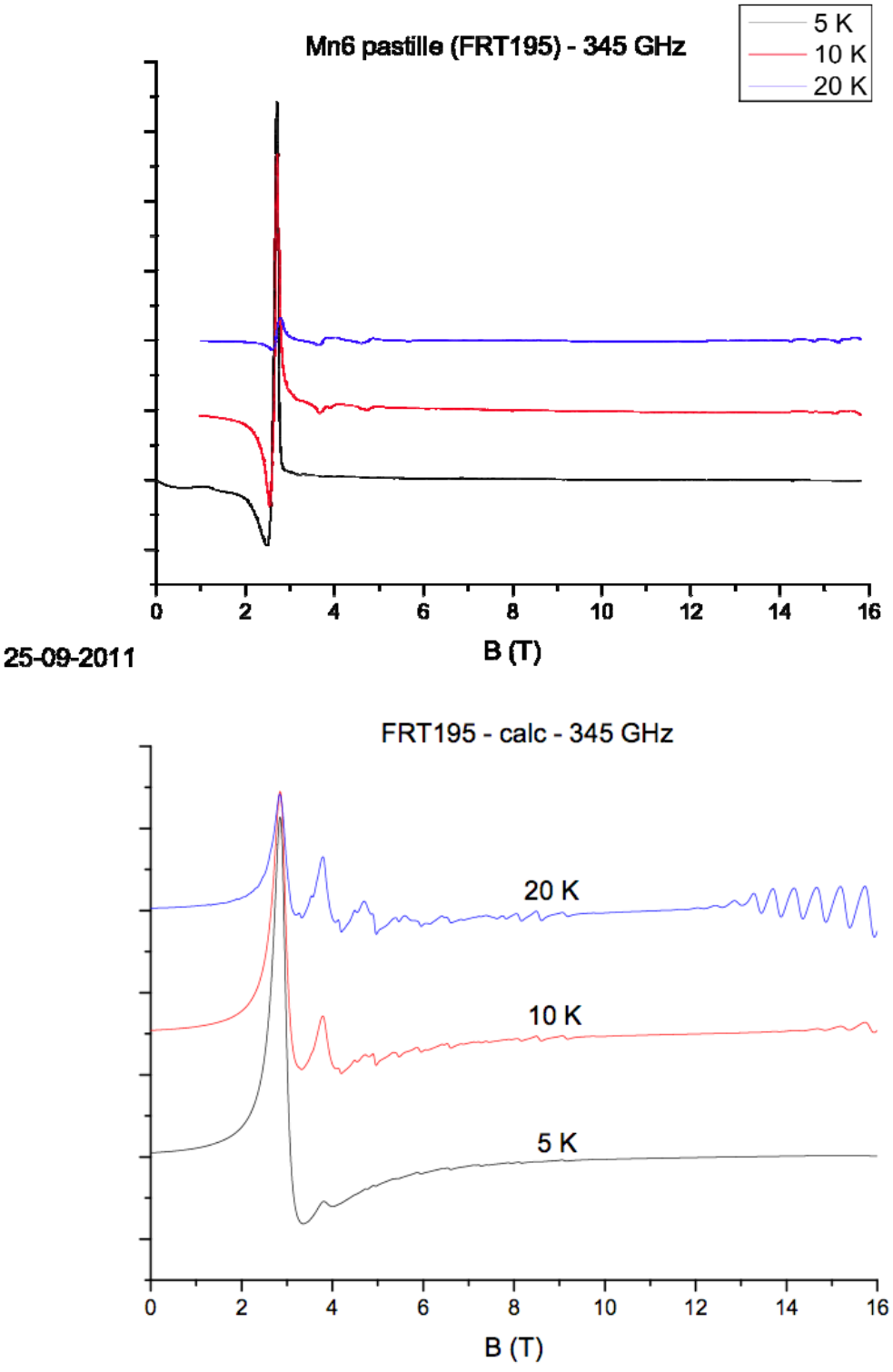

Fig. S35 Experimental (top) and calculated spectra for an $S = 12$ ground state (bottom) of **2'** at 345 GHz and T = 5, 10 et 20 K.

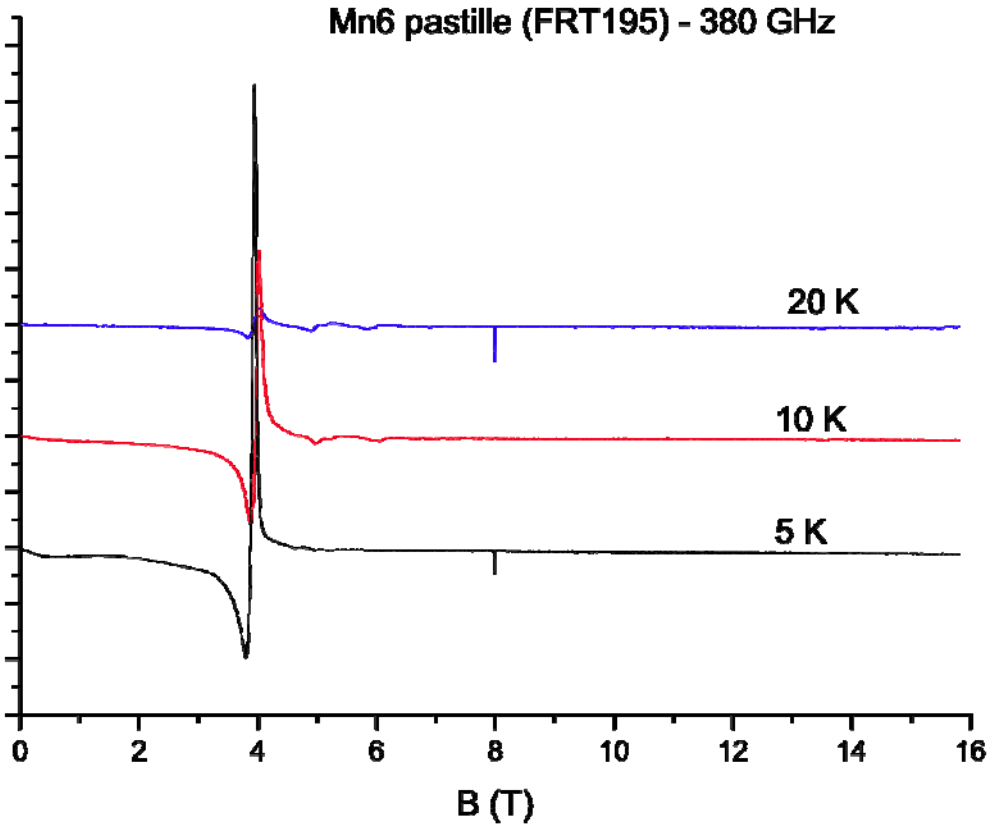
Mn6 pastille (FRT195) - 380 GHz
20 K
10 K
5 K
0
2
4
6
8
10
12
14
16
B (T)

24-09-2011

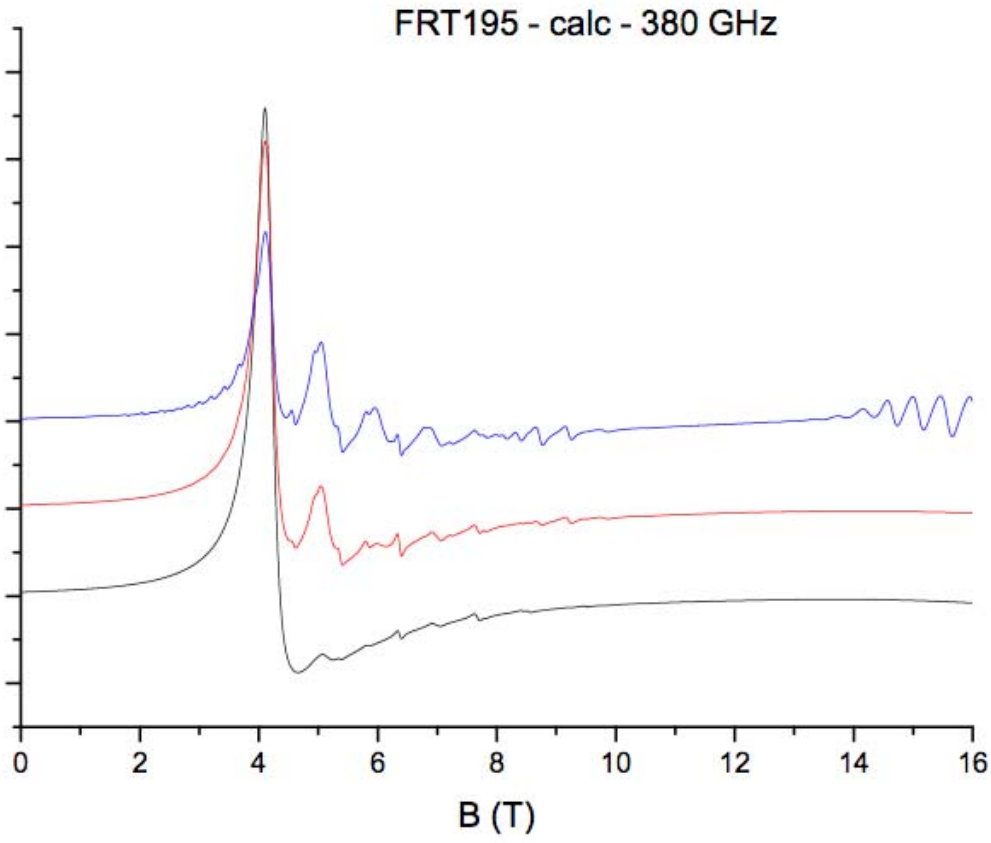
FRT195 - calc - 380 GHz
0
2
4
6
8
10
12
14
16
B (T)

Fig. S36 Experimental (top) and calculated spectra for an $S = 12$ ground state (bottom) of **2'** at 380 GHz and T = 5, 10 et 20 K.